Quantum oscillations in antiferromagnetic $CaFe_2As_2$ on the brink of superconductivity

N. Harrison[1], R. D.McDonald[1], C. H. Mielke[1], E. .D. Bauer[1], F. Ronning[1] and J. D. Thompson[1]
[1]*Los Alamos National Laboratory, MS-E536, Los Alamos, NM 87545*

(Dated: February 9, 2009)

We report quantum oscillation measurements on $CaFe_2As_2$ under strong magnetic fields− recently reported to become superconducting under pressures of as little as a kilobar. The largest observed carrier pocket occupies less than 0.05 % of the paramagnetic Brillouin zone volume− consistent with Fermi surface reconstruction caused by antiferromagnetism. On comparing several alkali earth AFe_2As_2 antiferromagnets (with A = Ca, Sr and Ba), the dependence of both the Fermi surface cross-sectional area F_α and the effective mass m^*_α of the primary observed pocket on the antiferromagnetic/structural transition temperature T_s is found to be consistent with quasiparticles in a conventional spin-density wave model. These findings suggest that a conventional spin-density wave exists within close proximity to superconductivity in this series of compounds, which may have implications for the microscopic origin of unconventional pair formation.

PACS numbers: 71.45.Lr, 71.20.Ps, 71.18.+y

The detection of magnetic quantum oscillations continues to be a powerful experimental method for determining the existence of Fermi surface reconstruction, often revealing the existence of small pockets of carriers [1, 2, 3] missed by other spectroscopic tools [4, 5]. In the recently discovered high T_c superconductors based on FeAs layers [6, 7, 8, 9, 10, 11], they have played an essential role in establishing the existence of a Fermi surface within the parent antiferromagnetic state [3, 12]. As with cuprates and heavy fermion systems [13], the proximity of antiferromagnetism to superconductivity raises the prospect of antiferromagnetically-mediated superconductivity.

Among stoichiometric AFe_2As_2 compounds, $CaFe_2As_2$ lies closest in pressure phase space to superconductivity (see Fig. 1)− reported to exist at pressures as low as 1.4 kbar [14, 15], compared to $\sim$ 30 kbar in its chemically closest relative $SrFe_2As_2$ [16]. One intriguing possibility therefore is that the optimal pressure p_s at which superconductivity occurs [14, 15, 16] is correlated with the spacing c between the bilayers (see Fig. 1) [18, 19, 20], which is in turn controlled by the size of the alkali earth ion A. The consecutive substitution of A with Ca, Sr and Ba thus provides a laboratory for relating possible c-dependent changes of the Fermi surface topology and antiferromagnetic correlations with the proximity to pressure-tuned superconductivity.

In the present paper, we determine the Fermi surface of $CaFe_2As_2$ by utilizing the contactless conductivity technique that has been successfully applied to $SrFe_2As_2$ [3] and $BaFe_2As_2$ [12], as well as the cuprate superconductors in strong magnetic fields [2, 21]. A sample of $CaFe_2As_2$ of dimensions $\approx 1 \times 1.5 \times 0.2$ mm^3 (preselected to have minimal Sn flux inclusion) is cut from a larger crystal and mounted with its tetragonal c axis aligned parallel to the magnetic induction $\mathbf{B} \approx \mu_0\mathbf{H}$ (or rotated away from $\mathbf{H}$ by an angle θ). Its planar face is attached to a 5 turn compensated coil of diameter ≈ 0.7 mm that forms part of a tunnel diode oscillator (TDO) circuit. The TDO resonates at a frequency of $\approx$ 46 MHz in the absence of an applied magnetic field, dropping by $\approx$ 200 kHz in $\sim$ 60 T in response to the magnetoresistivity of the sample. The associated increase in in-plane resistivity changes the coil inductance and resonance frequency, suggesting that the quantum oscillations (which

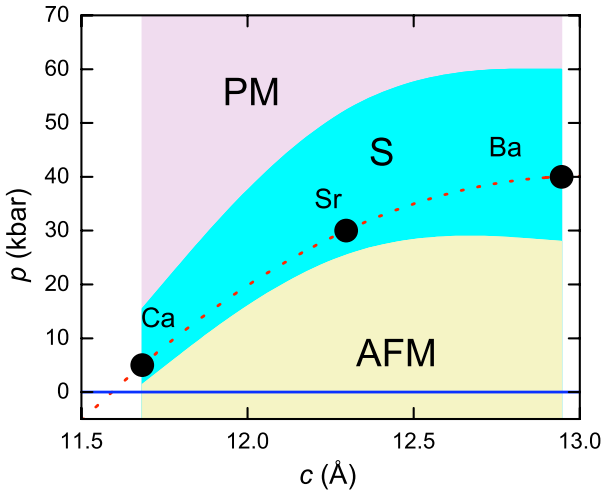

FIG. 1: Schematic pressure p versus FeAs bilayer spacing c diagram for AFe_2As_2 where A = Ca, Sr and Ba, indicating the nominal regions where antiferromagnetism (AFM), superconductivity (S) and possible paramagnetic metallic behavior (PM) reside. The black circles (and dotted line) represent the optimal pressure p_s at which superconductivity is reported to attain its highest value. The c values appropriate for the orthorhombic antiferromagnetic phase below T_s are taken from Refs. [18, 19, 20], while the p values are taken from Refs. [15, 16]. Lines are drawn between each of the compositions as guides for the eye. In $CaFe_2As_2$, the sensitivity of the competing antiferromagnetic and 'collapsed tetragonal' phases to shear associated with the pressure medium may play some role in fine-tuning superconductivity [17].

A	T_s (K)	F_α (T)	m^*_α (m_e)	F_γ (T)	m^*_γ (m_e)
Ca	170	395	1.8 ± 0.2	95	1.0 ± 0.2
Sr	200	370	2.0 ± 0.1	70	–
Ba	138	430	1.2 ± 0.3	95	0.9 ± 0.1

TABLE I: Values of the Fermi surface frequencies F_i and effective masses m_i for $\mathbf{H}\|\mathbf{c}$, taken from this work and Refs. [3, 12]. Also shown, is the structural transition temperature T_s into the orthorhombic, antiferromagnetic phase.

reach a maximum amplitude at ~ 60 T of 1 part in a 1000 of the magnetoresistance) originate from the Shubnikov-de Haas (SdH) effect. The TDO frequency is mixed down to < 1 MHz in two stages whereupon it is digitized at a rate of 20 MHz during the ~ 50 ms duration of the magnetic field pulse. The sample is immersed in gaseous or liquid ^{3}He throughout the experiments, with the temperature controlled through the vapor pressure for $T < 2$K or by a heater for $T > 2$K and measured using a calibrated cernox resistor (mounted close to the sample) immediately prior to the magnetic field pulse.

Figure 2 shows results of quantum oscillation experiments performed on $CaFe_2As_2$, after subtracting a linear background and performing Fourier transformation in $1/B$. When $\mathbf{H}\|\mathbf{c}$, several oscillations are discernable corresponding to a frequency $F_\alpha = 395 \pm 10$ T, with another feature at $F_\gamma = 95 \pm 20$ T becoming more clearly discernible at higher T when the amplitude of F_α is thermally suppressed (here we use the frequency labeling scheme adopted for $SrFe_2As_2$ in Ref. [3, 22]). A third frequency $F_\beta \sim 200$ T, if present, is strongly reduced in amplitude compared to that in $SrFe_2As_2$. On further performing a rotation study (presented in Fig. 3), both F_α and F_γ are found to be consistent with small ellipsoidal pockets in a similar fashion to $SrFe_2As_2$ [3], with the larger occupying less than 0.05 % of the paramagnetic Brillouin zone volume. These findings support a scenario in which the Fermi surface is reconstructed as a consequence of the broken translational symmetry brought about by magnetic ordering, as was recently established in $SrFe_2As_2$ [3].

A surprising result of the current study, however, is that the effective masses in $CaFe_2As_2$ exhibit only a small relative change compared to $SrFe_2As_2$ [3] or $BaFe_2As_2$ [12], in spite of $CaFe_2As_2$ being in much closer proximity to superconductivity in Fig. 1. Figure 4 shows a fit of the Lifshitz-Kosevich theoretical [23] form $A = A_0 X/\sinh X$ (where $X = 2\pi^2 m_i k_B T/\hbar e B$) to the temperature-dependent quantum oscillation amplitude in $CaFe_2As_2$. The fitted values of the effective mass are compared to those of similar pockets in $SrFe_2As_2$ and $BaFe_2As_2$ in Table I and Fig. 5.

The absence of a divergence in the effective mass on reducing c in Fig. 5a, or reducing the antiferromagnetic/structural transition temperature T_s in Fig. 5b, is in marked contrast to recent observations made in heavy fermion antiferromagnets [24] and cuprate superconductors [25], where subtle changes in p or doping lead to

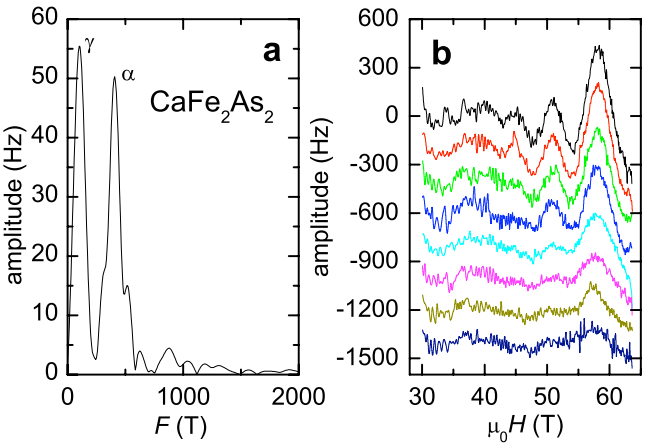

FIG. 2: **a** Fourier transform of quantum oscillations in the TDO resonance frequency in $1/B$ at 0.98 K. **b** Raw TDO frequency oscillations for $\mathbf{H}\|\mathbf{c}$ with curves at $T = 0.98$, 1.52, 2.08, 3.1, 4.2, 5.0, 6.0 and 7.0 K consecutively offset.

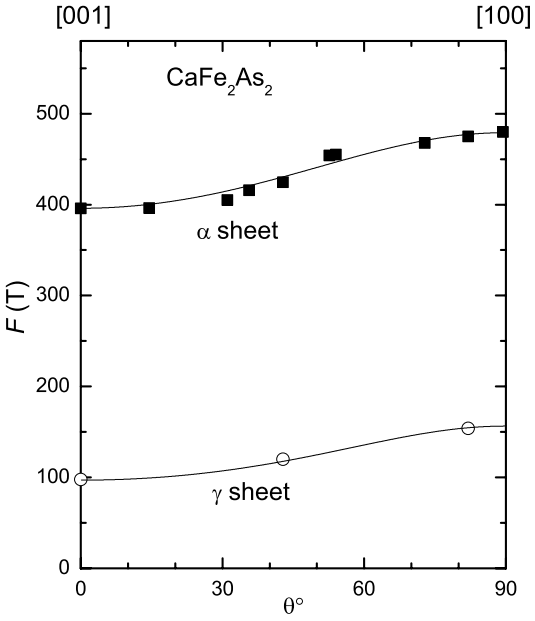

FIG. 3: Magnetic field orientation-dependence of the α and γ quantum oscillation frequencies determined by Fourier transformation, where $\theta = 0$ corresponds to $\mathbf{H}\|\mathbf{c}$ and $\theta = 90°$ corresponds to $\mathbf{H}\|\mathbf{a}$ at room temperature. The sample and coil are rotated in-situ.

marked changes in m^*. Given that the Fermi velocities and.or effective masses are renormalized by only a factor a two compared to bandstructure estimates [3, 12], one possibility is that the physics of AFe_2As_2 is much closer to that of a conventional spin-density wave [26], with the on-site Coulomb repulsion between the d-electrons being insufficiently strong to cause development of a Mott insulating state. In the case of a conventional spin-density wave, antiferromagnetic correlations lead to a comparatively weak enhancement of m^* that increases with the

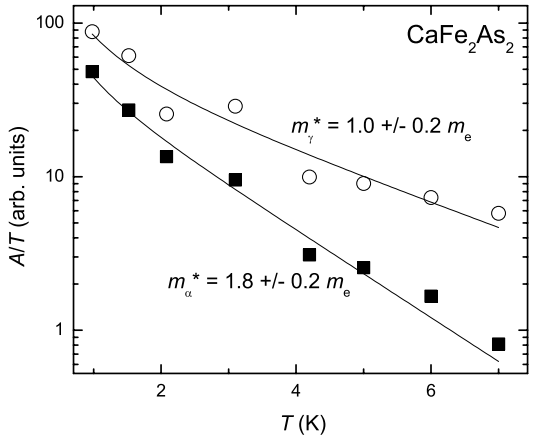

FIG. 4: Temperature-dependence of A/T for $\mathbf{H}\|\mathbf{c}$ together with fits to the Lifshitz-Kosevich theory as described in the text. Fitted values of the effective mass are shown, where m_e is the free electron mass.

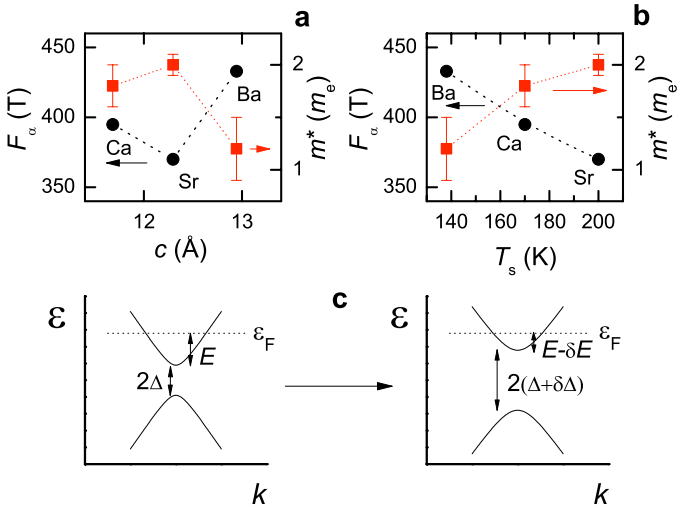

FIG. 5: Plots of the largest quantum oscillation frequency F_α for $\mathbf{H}\|\mathbf{c}$ (right-hand axis) and effective mass m^*_α (left-hand-axis) versus the bilayer spacing (**a**) and the structural transition temperature T_s (**b**) from the high temperature tetragonal phase into the low temperature orthorhombic, antiferromagnetic phase. **c**, a one-dimensional schematic showing how the size of the pocket ($\propto F$) is inversely related to the size of the spin-density wave gap ($2\Delta \propto T_s$). In the simplest model, an increase $\delta\Delta$ in Δ leads to an equal and opposite reduction δE in the filling E of the pocket (for a constant Fermi energy ε_F).

size of the spin-density wave gap 2Δ [27]. Differences in the electronic structures of the pnictides, cuprates and heavy fermions may account for some of their differences in behavior. For example, the electronic structure of FeAs layered compounds differs from the others in that multiple (d-electron) bands cross the Fermi energy in the unreconstructed tetragonal phase [3, 28]. Strong on-site Coulomb repulsion operating within a single d- or f-electron band in heavy fermion and high T_c cuprates, by contrast, makes those systems vulnerable to Mott insulating behavior (in which the d- or f-electrons no longer contribute to the electrical conduction) [29, 30], providing a possible route for the divergence of m^* inside their antiferromagnetic states.

Evidence for conventional spin-density wave ordering in $A\mathrm{Fe_2As_2}$ is provided in Fig. 5b by the reduction in the size of the pocket F_α and weak enhancement of m^*_α on increasing T_s (which varies non-monotonically with A and c). Here, we concentrate on the larger pocket that is observed consistently in all antiferromagnetic $A\mathrm{Fe_2As_2}$ compounds, which also contributes most to the electronic heat capacity on account of its larger surface area. The observed trends in Fig. 5b can be understood by considering a simplified spin-density wave reconstruction model (see Fig. 5c) in which the spin-density wave gap 2Δ is proportional to the transition temperature T_s in accordance with the BCS description $\Delta = 1.76 k_B T_s$ [31]. If the unreconstructed Fermi surfaces are assumed to be similar throughout [3], the progressive increase in 2Δ incurred on going from Ba to Ca to Sr improves the degree of nesting, resulting in a progressive reduction in the sizes of the pockets and a gradual flattening of the reconstructed band leading to the enhancement in m^*.

Quantitative consistency with the spin-density wave model can be tested by comparing the reduction δE in the filling E of the pocket with the increase $\delta\Delta$ in Δ on going from A = Ca to Sr (which have the smallest percentage error bars in m^*_α). If we assume a parabolic dispersion whereby $E = \hbar e F_\alpha / m^*_\alpha$ and a BCS gap, we arrive at quantitatively similar incremental changes $\delta E \approx 4 \pm 2$ meV and $\delta\Delta \approx 4.5$ meV as expected for the simple spin-density wave model presented in Fig. 5c.

While spin-density wave physics seems to be relevant to this series of compounds, the process by which it is destabilized under pressure, leading to the emergence of superconductivity, is not yet clearly established. Hydrostatic pressure applied to $\mathrm{CaFe_2As_2}$ was recently shown to cause a first order transition at $p_c \approx 3.5$ kbar into a 'collapsed tetragonal phase' with the same crystal symmetry as the room temperature ambient pressure phase but with a greatly reduced lattice spacing c [18]. Importantly, the collapsed tetragonal phase has a ~ 6 % reduced volume compared to both the room temperature/ambient pressure tetragonal and orthorhombic phases, and has significantly different lattice parameters. It was recently argued by Yu *et al.* that by using a pressure medium that solidifies at a higher T than ^{4}He, ideal hydrostatic pressure conditions are less likely to be maintained [17]. One possible outcome is that a near-continuous transformation in volume occurs with p under such conditions, leading to phase separation in which orthorhomic and collapsed tetragonal domains coexist, with shear forces enabling both of them to exist out of equilibrium. It is under these circumstances that superconductivity is reported to exist in $\mathrm{CaFe_2As_2}$ [14, 15, 17].

While neutron scattering experiments have yet to be

performed on $SrFe_2As_2$ and $BaFe_2As_2$ under high pressures to verify whether the transition into a collapsed tetragonal phase is universal, the proximity to such a phase in $CaFe_2As_2$ by virtue of its reduced c may be an important factor in the relative ease by which superconductivity can be tuned [18]. The sensitivity of the superconducting volume fraction in $SrFe_2As_2$ and $BaFe_2As_2$ to pressure provides some hint of a phase separation scenario analogous to that in $CaFe_2As_2$ [3]. Identifying which of the phases is primarily responsible for the observed superconductivity in $CaFe_2As_2$ and the directionality of the shear required for its optimization remains a formidable challenge.

The discontinuous nature of the transition into the collapsed tetragonal phase with a greatly reduced bilayer spacing compared to the FeAs-layered compounds with higher T_c's, suggests that the transition itself is unlikely to be a source of diverging antiferromagnetic fluctuations. An alternative possibility is that superconductivity emerges from within the orthorhombic phase by way of a continuous suppression of antiferromagnetism by shear-restored geometric frustration of the staggered Fe moments or by disorder. This would yield a quantum critical point qualitatively different [35] from that usually associated with pressure-tuned superconductivity in heavy fermion compounds [24, 26, 29]. A large spacing between the layers is preserved in the orthorhombic phase, which appears to be an important factor in attaining high superconducting transition temperatures in FeAs layered compounds [32], as it is in other layered superconductors [33, 34].

In summary, while there remains uncertainty over the precise conditions required to optimize superconductivity with pressure, $CaFe_2As_2$ is arguably the stoichiometric antiferromagnet existing within closest proximity to superconductivity. A comparison of the Fermi surface properties of $CaFe_2As_2$ with those of $SrFe_2As_2$ and $BaFe_2As_2$ reveals that the effective masses and pocket sizes exhibit a dependence on the antiferromagnetic/structural transition temperature T_s, that is consistent with weakly enhanced quasiparticles moving in an antiferromagnetic background of spins. These findings suggest that antiferromagnetism in AFe_2As_2 can be effectively understood from the perspective of a conventional spin-density wave– likely placing constraints on possible mechanisms for superconductivity in FeAs layered compounds [13, 29, 35].

This work is conduced under the auspices the US Department of Energy, while the National High Magnetic Field Laboratory, where the experiments were conducted, is primarily funded by the National Science Foundation and the State of Florida.

[1] N. Doiron-Leyraud *et al.*, Nature **447**, 565 (2007).
[2] E. A. Yelland *et al.*, Phys. Rev. Lett. **100**, 047003 (2008).
[3] S. E. Sebastian *et al*, J. Phys.: Cond. Matt. **20**, 422203 (2008).
[4] M. A. Hossain *et al.*, Nature Phys. **4**, 527 (2008).
[5] H. Y. Liu *et al.*. Phys. Rev. B **78**, 184514 (2008).
[6] Y. Kamihara, *et al.*, J. Am. Chem. Soc. **130**, 3296 (2008).
[7] H. Takahashi *et al.*, Nature **453**, 376 (2008).
[8] X. H. Chen *et al.*, Nature **453**, 761 (2008).
[9] Z.-A. Ren *et al.*, Europhys. Lett. **82**, 57002 (2008); Z.-A. Ren *et al.*, Materials Research Innovations **12**, 106 (2008).
[10] R. H. Liu *et al.*, Phys. Rev. Lett. **101**, 087001 (2008).
[11] I. I. Mazin *et al.*, Phys. Rev. Lett. **101**, 057003 (2008).
[12] J. G. Analytis *et al.* <http://arXiv.org/abs/0902.1172>.
[13] P. Monthoux, D. Pines and G. G. Lonzarich, Nature **450**, 1177 (2007).
[14] M. S. Torikachvili *et al.*, Phys. Rev. Lett. **101**, 057006 (2008).
[15] T. Park *et al.*, J. Phys. Con.: Matt. **20**, 322204 (2008); H. Lee *et al.*, <http://arXiv.org/abs/0809.3550>.
[16] P. Alireza, *et al.*, J. Phys.: Cond. Matt. **21**, 012208 (2009).
[17] W. Yu *et al.*, <http://arXiv.org/abs/0811.2554>.
[18] A. Kreyssig *et al.*, Phys. Rev. B **78**, 184517 (2008).
[19] M. Tegel *et al.*, J. Phys. Cond.: Matt. **20**, 452201 (2008).
[20] M. Rotter *et al.*, Phys. Rev. B **78**, 020503 (2008).
[21] S. E. Sebastian, *et al.* Nature **454**, 200 (2008).
[22] Note that the α and β are mistakenly interchanged in Fig. 2b of Ref. [3] and in the discussion section of Ref. [3] relating the pockets to the bandstructure calculations.
[23] D. Shoenberg, *Magnetic oscillations in metals* (Cambridge University Press, Cambridge, 1984).
[24] H. Shishido *et al.*, J. Phys. Soc. Japan **74**, 1103 (2005).
[25] S. E. Sebastian *et al.*, Workshop on cuprate fermiology, Maryland (2008).
[26] J. A. Hertz, Phys. Rev. B **14**, 1165 (1976); A. J. Millis, Phys. Rev. B **48**, 7183 (1993).
[27] R. D. McDonald *et al.*, Phys. Rev. Lett. **94**, 106404 (2005).
[28] D. J. Singh, and M. H. Du, Phys. Rev. Lett. **100**, 237003 (2008).
[29] Q. Si *et al.*, Nature **413**, 804 (2001).
[30] M. Imada, A. Fulimori, and Y. Tokura, Rev. Mod. Phys. **70**, 1039 (1998).
[31] G. Grüner, *Density waves in solids, Frontiers in physics* **89** (Addison-Wesley, 1994).
[32] M. Rotter, M. Tegel, and D. Johrendt, Phys. Rev. Lett. **101**, 107006 (2008); K. Sasmal *et al.*, Phys. Rev. Lett. **101**, 107007 (2008).
[33] J. R. Schrieffer, J. S. Brooks (Eds.), *High-temperature superconductivity theory and experiment* (Springer Science, 2007).
[34] E. D. Bauer *et al.*, Phys. Rev. Lett. **93**, 147005 (2004).
[35] Q. Si and E. Abrahams, <http://arXiv.org/abs/0804.2480>